A stereotaxic image-guided surgical robotic system for depth electrode insertion

Fanle Meng, Hui Ding, and Guangzhi Wang*, *Member, IEEE*

***Abstract*— This article constructs a surgical robotic system for the stereotactic insertion of the depth electrodes for stereoelectroencephalogram (SEEG). The purpose is to increase the efficiency of the stereotactic insertion of the electrodes. The registration method of this system is based on the noninvasive fiducial markers. After registration, the robotic system can locate all the preplanned electrode trajectories automatically. The validation of this proposed system has been performed by testing the time consumption of the system workflow and measuring the positioning accuracy on phantoms. From the result, we conclude that this surgical robotic system can assist surgeons in performing the stereotactic insertion of the depth electrodes accurately and efficiently.**

I. Introduction

For a quantity of people with medically intractable epilepsy, whose epileptic seizures cannot be controlled with medication, surgical intervention can completely eliminate their disability [1]. Accurate localization of the epileptogenic zone is one of the key factors in the effective surgical treatment as well as the reduction of complication. Recent years, the stereoelectroencephalogram (SEEG) method, proposed by Talairach and Bancaud [2], is widely used as a preoperative assessment of the epileptogenic zone localization [3]. This technique provides three-dimensional (3D) information about the epileptic seizures by using numerous electrodes which include the multi contact electrodes to perform intracranial recording [4]. The insertion of SEEG depth multi contact electrodes can be performed via minimally invasive surgery procedure without craniotomy which has a high-risk occurrence of complication [5].

Both stereotactic techniques and surgical navigation techniques have been used to assist the minimally invasive surgery of depth electrodes insertion. Before surgery, accurate surgery plan is made on the preoperative images to determinate the trajectories of multi contact electrodes. During the surgery, when using a stereotactic frame to guide the surgery, after the preplanned trajectories coordinates transformed into the frame space from the image space, surgeons adjust the frame manually to locate each preplanned electrode trajectory. As for using the optical tracking navigation system to assist SEEG depth electrodes insertion, after a registration procedure between the image space and the patient space performed, the electrode trajectories need to be aligned by a real-time pointer tool on the preoperative image and then be located manually one after another. Since numerous electrodes need to be inserted in the SEEG depth electrodes insertion surgery, both methods mentioned above are relatively time-consuming and strenuous.

In the depth electrodes insertion surgery, the shortcomings referred above can be overcome efficiently by using robots to locate the preplanned electrode trajectories within less time. There have been researches on the stereotactic surgical robotic system for depth electrodes insertion. And the registration methods include using a stereotactic frame or an ultrasonic localizer to conduct the registration [6], and scanning the patient's head with an optical distance sensor coupled to the robot arm [7]. Based on the registration, the robot locates the preplanned electrodes trajectories.

Taking the requirement of SEEG depth electrodes insertion surgery into account, we constructed a stereotactic surgical robotic system. The registration method is based on the noninvasive fiducial markers. After a registration step performed, the robotic system can locate all the electrode trajectories automatically and adjust to a configuration suitable for surgeons' operation. The experiments on phantoms indicate that this system is convenient to operate. Moreover it provides a time-saving method of locating electrode trajectories with the similar accuracy of optical surgical navigation system.

II. Methods

The surgical robotic system proposed in this article mainly includes three parts, which are a multi-axis robot arm with a controller, an optical tracking sensor with tracking tools and a software, as shown in Fig. 1. The optical tracking sensor Polaris Spectra（NDI, Canada) with an accuracy of 0.25mm is used to position the tracking tools, including a pointer tool and

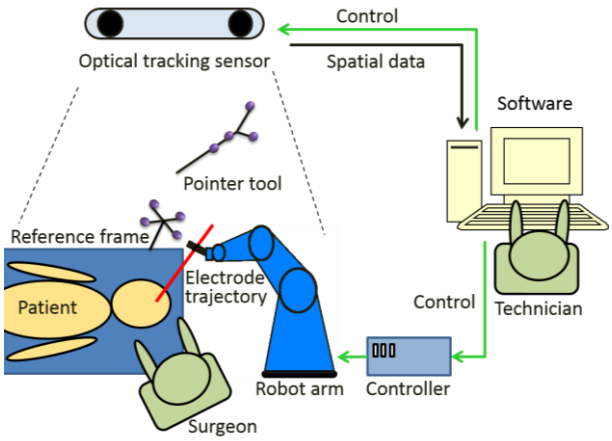

Figure 1. The components of the robotic system

This work was supported by the National Key Technology Support Program of China and Beijing（2012BAI16B03，Z131100006413027）.

Fanle Meng (mengfanle@gmail.com) , Hui Ding (dinghui@tsinghua.edu.cn) , and Guangzhi Wang (wgz-dea@tsinghua.edu.cn) are all with the Department of Biomedical Engineering, Tsinghua University, Beijing 100084, China (phone: 8610-62783631; fax: 8610-62794377).

a reference frame, in order to pick the fiducial points on patient's head and on the robot arm end-effector during the registration step. Combined with the fiducial markers on the preoperative magnetic resonance imaging (MRI) and/or computed tomography (CT) images, the software makes some spatial transformation in order to map the preplanned electrode trajectories on the images into the patient space then transforms them into the robot arm space. Thus, the software controls the robot arm to locate the orientation of the electrodes and relative surgical instrument. The system workflow is shown in Fig. 2 and the registration and location parts in the workflow will be described in detail below.

A. Registration

The registration step is to get the coordinate transformations of the image coordinate $\{I\}$, the patient coordinate $\{Re\}$ and the robot arm coordinate $\{R\}$ in order to transform the electrode trajectories from $\{I\}$ to $\{R\}$. As is shown in Fig. 2, the registration that is based on fiducial points includes patient registration and robot arm registration. The fiducial points for the patient registration are the skin markers pasted on the patient's head before the image acquisition. And the fiducial points for robot arm registration are several positions of the robot arm end-effector. The transform matrix T between two coordinates is calculated by point-pair matching. Let ${}^{R}_{I}T$ be the transform matrix from $\{I\}$ into $\{R\}$ and so on. Therefore ${}^{R}_{I}T$ can be calculated in (1) and the transformation process is illustrated in Fig. 3:

$$ {}^{R}_{I}T = {}^{R}_{Re}T \cdot {}^{Re}_{I}T \tag{1} $$

The target points and entrance points of the trajectories, namely ${}^{I}p$, in $\{I\}$ can be mapped into $\{R\}$ denoted by ${}^{R}p$ through:

$$ {}^{R}p = {}^{R}_{I}T \cdot {}^{I}p \tag{2} $$

The transformation in this system is centering on the patient coordinate which is described by the reference tool attached on the holder of patient's head and do not shift relative to the head during the whole surgery. Fiducial points are all picked by the pointer tool in the reference frame coordinate. Thus, during the procedures of picking points, the optical tracking sensor can be moved in order that the tracking tools are all in the vision field without being obstructed by other objects in the operation room (OR).

B. Robot arm location and configuration adjustment

To locate the electrode trajectories by the robot arm, a guidance module attached on the end-effector is designed for

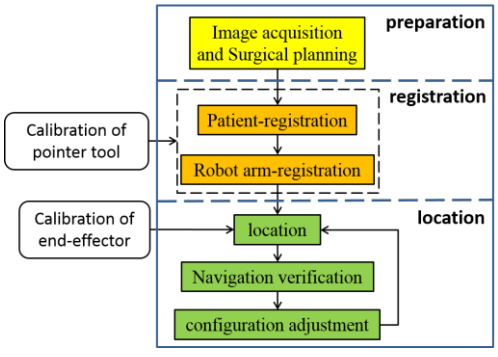

Figure 2. The system workflow

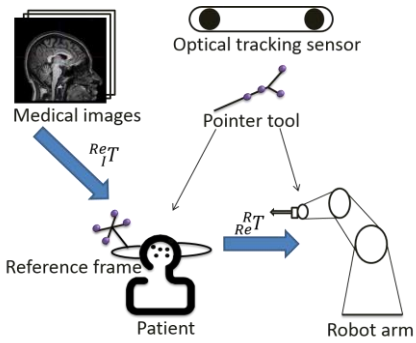

Figure 3. Registration transformation

constraint the orientation of the electrodes and surgical instruments (A in Fig. 5). After the registration step, each electrode trajectories has been mapped into the robot arm coordinate. The robot arm end-effector locates the electrode trajectories according to the robot inverse kinematics which refers to transform the given position and orientation of the end-effector to each joint angel. To enhance the safety of the operation, the guidance module is optically tracked and the located orientation is displayed on the preoperative images before electrode insertion to verify if the location is correct. Also, a stop button is designed as a hardware safety installation to stop the motion immediately when accidents will occur.

A robot arm with six degrees of free (DOFs) is selected to construct this surgical robotic system rather than the five DOFs for the task of locating electrode trajectories. In this case, there is a redundant DOF: the rotation around the orientation of electrode insertion, defined as the z-axis of the end-effector coordinate (A in Fig. 5). Thus, there are numerous solution set of the joints angle for locating a given electrode orientation based on the inverse kinematics. To get enough operation space for surgeons, avoiding the obstruction of the mechanical structure of the robot arm, the configuration can be adjusted without changing the given orientation because of the redundant DOF. When surgeons guide the system by the pointer tool, the robot arm relocates the same orientation with a new configuration through the optical tracking information. Similarly, with the redundant DOF, the guidance module can approach patient's head along the insertion orientation. Therefore, when drilling the skull, the guidance module is used not only to constraint the orientation but also to control the stepping of the twist drill without other device, which simplifies the surgical procedures such as disinfection and installation.

III. Validation

To validate the efficiency of this surgical robotic system for SEEG depth electrodes insertion, we measured the time consumption of the key steps in the system workflow with a skull phantom in the lab environment. Then, we designed experiments to test the positioning accuracy and analyze the factors affecting the positioning accuracy.

A. Time consumption test of the workflow

First, CT images of the skull phantom were scanned after 6 fiducial markers were pasted on it, then 12 depth electrode trajectories were planned based on the reconstructed 3D scalp surface and image slices (Fig. 4). The phantom was fixed on

the head holder. Then an inexperienced person performed the patient registration step by picking the fiducial markers successively under our direction. The end-effector moved to 4 different positions as fiducial points which were picked automatically to perform the robot arm registration. After the electrode trajectories were mapped into the robot arm coordinate, the end-effector moved and located all the trajectories one by one. The end-effector was tracked to ensure the correct location when each location step finished (Fig. 4).

We recorded the time spent on the patient registration, the robot arm registration, the trajectories transformation and the location of each trajectory. In particular, the time spent on one location step referred to the duration between the end-effector starting to depart from the previous trajectory and completing the verification by optical tracking after locating the current trajectory.

B. *Positioning accuracy experiment*

An organic glass phantom (B in Fig. 5) was designed with the similar scale of human head to test the positioning accuracy of this surgical robotic system. A set of locating pits are distributed on the phantom. The CT images of the phantom were scanned through the Siemens CT scanner with the resolution of 512×512, the pixel spacing of 0.32m ×0.32mm and the slice thickness of 0.7mm, 3D visualization (C in Fig. 5). Fiducial markers for registration were 8 pits on the outer wall of the phantom and 13 electrode trajectories were planned shown as lines: the pits on the top of the slender columns were the target points while the entrance points were presented as spheres. The experiment setup is shown in Fig. 5. In the experiment, the phantom was fixed on the head holder instead of the patient's head. A high accuracy optical tracking sensor Optotrak (NDI, Canada) is used as a position measuring tool. Let P_i be the position of each target point in the physical space picked by Optotrak which was seen as the real position. The target point was touched by pointer tool slightly. After the registration step performed, the robot arm located each electrode trajectory. Let R_i be the position of each located target point picked by Optotrak which was positioned by the end-effector when it stopped moving. The positioning error $Error_{pos}$ is defined as the mean distance between P_i and R_i:

$$Error_{pos} = \frac{1}{n}\sum_{i=1}^{n}\|R_i - P_i\| \quad (3)$$

where n is the amount of the available electrode trajectories.

Each part of the system shown in Fig. 2 was considered to affect the positioning accuracy. We analyzed the mainly three parts which are the operation of preoperative images, the optical tracking sensor Polaris and the robot arm. In the system workflow, the operation of images includes picking fiducial markers and planning the electrodes trajectories. We combined Polaris and the robot arm to be a new positioning system and tested its positioning error, and compared the error with the positioning error of the whole surgical robotic system. Then, we evaluated the error affected by the optical tracking sensor. The optical tracking sensor Optotrak took the place of Polaris to be combined with the robot arm to be another positioning system. Finally, we considered that certain error was contributed by the robot arm and studied the error related to the end-effector.

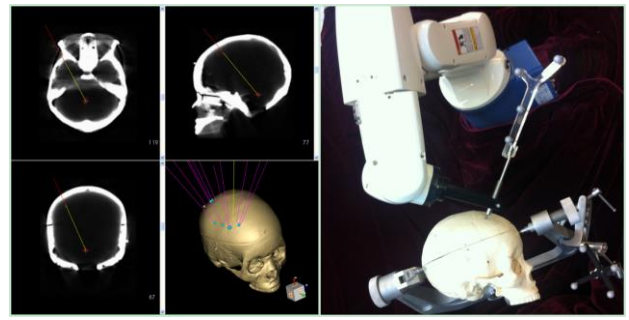

Figure 4. The time consumption test setup. Left: the CT image of the skull and the design of trajectories. Right: the robot arm located one of the trajectory and the end-effector was tracked.

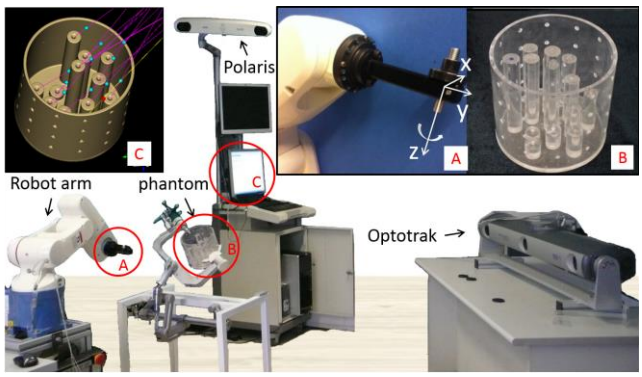

Figure 5. The positionning accuracy experiment setup. The guidance module is the robot arm end-effector shown in detail in A, the photograph of the phantom is shown in B and the design of trajectories on the 3D visualization of the phantom is shown in C.

1) *The positioning error experiment of the system constructed by optical tracking sensor and the robot arm*

After fixing the organic glass phantom on the head holder, the positions of the target points in the physical space were picked by both the Polaris and Optotrak. Let $Real_i$ be each position in Optotrak space which is seen as the real position of the target point while the positions in the Polaris space is seen as the target point of the preplanned trajectory. The trajectories were planned in the Polaris space and the robot arm registration step was performed to map these trajectories into the robot arm space. Then the end-effector positioned the target points. At last, let Pos_i be each located position picked by Optotrak and compared with the real positions. The positioning error of this new system was calculated by (4),

$$Error_{opt-rob} = \frac{1}{n}\sum_{i=1}^{n}\|Pos_i - Real_i\| \quad (4)$$

where n is the amount of the available electrode trajectories.

Then, to study the error contributed by Polaris, Polaris was replaced by Optotrak and the experiment described above repeated.

2) *The error test related to the robot arm end-effector*

In the robot arm registration step, the pointer tool is inserted into the guidance module to pick the fiducial positions. Because the connection of the pointer tool and the guidance module is not rigid connection, there is certain shake to increase the repeated positioning error which may affect the accuracy of registration. We inserted the pointer tool into the guidance module and move the robot arm end-effector to position a same point for 7 times and pick the located positions by Optotrak. We chose 3 different points to repeat this test for a mean value.

IV. Result and Discussion

A. Time consumption of the workflow

The time spent on each item was shown in TABLE I. The total time consumption of locating all the 12 depth electrode trajectories was less than 6 minutes, even the time of the whole workflow is not much, which meant that this robotic system provided an efficient solution for locating the preplanned electrode trajectories. The duration of the surgery involving the robotic system is expected to be measured to compare with the traditional surgery after it is used in the OR in the future.

Considering the safety of surgery, we set a low speed for the robot arm and the end-effector went back to an initial position between two location steps of electrode trajectories. The motion speed and the distance between the initial position and the target position is the main factors in affecting the location time consumption. Effective methods used in robot motion planning will make the robot arm to move the next location directly in order to decrease the location time.

TABLE I. Time Consumption of the Workflow

	Time Consumption			
Test items	***Patient registration***	***Robot arm registration***	***Trajectories transformation***	***Trajectories location***
time consumption	2min	1min	10.1s	<6min

B. Positioning error

To validate the stability of the positioning error, four operators performed the positioning accuracy experiment for several times, among whom, a person performed for 4 times while the others performed once. The result was shown in TABLE II. The positioning accuracy of this surgical robotic system for depth electrodes insertion achieves the similar level of the optical surgical navigation system [8, 9].

TABLE II. Positioning Error

	Positioning error						
Operator	***A_1***	***A_2***	***A_3***	***A_4***	***B***	***C***	***D***
Mean(mm)	2.22	1.23	1.21	1.58	1.79	1.67	2.32
STD(mm)	0.37	0.38	0.66	0.98	0.72	0.22	0.41

1) The positioning error experiment of the system constructed by optical tracking sensor and the robot arm

The positioning error of the system constructed by Polaris and the robot arm was 1.16 ± 0.38mm, which was slightly smaller than that of the whole system. It was indicated that the operation of picking fiducial markers and planning electrode trajectories on the images had an effect on the positioning accuracy, but not obviously. The experience of performance may reduce the affection.

The positioning error of the system constructed by Optotrak and the robot arm was 0.62 ± 0.23mm. Comparing these two positioning errors, we could see that the optical tracking sensor contributed certain error to the whole system, but the error was accessible. Also, considering the portable and less expensive characteristic, we select Polaris as the optical tracking sensor to construct the robotic system rather than Optotrak with large volume, high cost and wired markers that are not convenient to use in the OR.

2) The error related to the robot arm end-effector

The result of repeated positioning error was 0.26 ± 0.15mm, which was much larger than that given by the manufacturer of the robot arm. This error affected not only the accuracy of the robot arm registration but also the precision of measurement in the positioning accuracy experiment. Improvement on the connection of the pointer tool and the guidance module could reduce this error.

Similarly, in the location step of the workflow, the calibration error of the end-effector coordinate, which attached on the guidance module, is a main factor that affected the positioning accuracy. The calibration is based on the dimension and installment position of the guidance module, so the calibration error depends much on the machining precision.

V. Conclusion

For the SEEG depth electrode trajectories insertion surgery, this article proposes a stereotactic surgical robotic system to locate the preplanned trajectories automatically. We tested the time consumption of the workflow and the positioning accuracy, then analyzed the factors affecting the accuracy. In conclusion, this surgical robotic system provides a convenient and time-saving method for the guidance of SEEG multi electrodes insertion and has reached the positioning accuracy of optical surgical navigation system. To be used in the OR, there are some improvements to be done on this surgical robotic system. For instance, more constraints should be considered in the future work to enhance the safety.

References

[1] J. Engel Jr, "Surgery for seizures," New England Journal of Medicine, vol. 334, pp. 647-653, 1996.

[2] J. Talairach and J. Bancaud, "Stereotaxic approach to epilepsy. Methodology of anatomo-functional stereotaxic investigations," Prog Neurol Surg, vol. 5, pp. 297-354, 1973.

[3] W. Liu, H. Guo, X. Du, W. Zhou, G. Zhang, H. Ding, et al., "Cortical vessel imaging and visualization for image guided depth electrode insertion," Computerized Medical Imaging and Graphics, vol. 37, pp. 123-130, 2013.

[4] A. Olivier, W. W. Boling, and T. Tanriverdi, Techniques in epilepsy surgery: the MNI approach: Cambridge University Press, 2012.

[5] J. V. Rosenfeld, "Minimally invasive neurosurgery," Australian and New Zealand journal of surgery, vol. 66, pp. 553-559, 1996.

[6] Q. H. Li, L. Zamorano, A. Pandya, R. Perez, J. Gong, and F. Diaz, "The application accuracy of the NeuroMate robot — A quantitative comparison with frameless and frame - based surgical localization systems," Computer Aided Surgery, vol. 7, pp. 90-98, 2002.

[7] S. Ferrand-Sorbets, M. Delphine Taussig, M. Fohlen, C. Bulteau, G. Dorfmuller, and O. Delalande, "Frameless stereotactic robot-guided placement of depth electrodes for stereo-electroencephalography in the presurgical evaluation of children with drug-resistant focal epilepsy," in CNS Annual Meeting, 2010.

[8] A. D. Mehta, D. Labar, A. Dean, C. Harden, S. Hosain, J. Pak, et al., "Frameless stereotactic placement of depth electrodes in epilepsy surgery," Journal of neurosurgery, vol. 102, pp. 1040-1045, 2005.

[9] M. Murphy, T. O'Brien, and M. Cook, "Insertion of depth electrodes with or without subdural grids using frameless stereotactic guidance systems--technique and outcome," British journal of neurosurgery, vol. 16, pp. 119-125, 2002.